

NUMERICAL ANALYSIS OF AERODYNAMIC CHARACTERISTICS OF A BUMPED LEADING EDGE TURBINE BLADE

Z. Čarija^{1*} – E. Marušić² – Z. Novak³ – S. Fućak⁴

¹Department of Fluid Mechanics, Faculty of Engineering, University of Rijeka, Vukovarska 58

²Faculty of Engineering, University of Rijeka, Vukovarska 58

³Polytechnic of Rijeka, Vukovarska 58

⁴Department of Thermodynamics and Energy Engineering, Faculty of Engineering, University of Rijeka, Vukovarska 58

ARTICLE INFO

Article history:

Received: 12.7.2013.

Received in revised form: 11.12.2013.

Accepted: 12.12.2013.

Keywords:

Wind turbine blade

Aerodynamics

Humpback whale

Bumped leading edge

Renewable energy

Abstract:

This paper investigates the aerodynamic effects of waving bumps inspired by a humpback whale fin on the leading edge of a turbine blade. A comparison was made between performances of two isolated blades: a blade with a sinusoidally shaped bumped leading edge (LE) and one with a straight leading edge; both based on the same NACA0012 cross section profile.

The simulations used a Reynolds number of $1.8 \cdot 10^5$ for a range of angles of attack from 0° to 30° . The results for the bumped blade have shown a substantial gain in aerodynamic characteristics for certain angles of attack (AoA). At AoA larger than 10° , the bumped blade has shown an increase in lift (3%-9.5%) and decreased drag, while negligible differences in lift and a smaller drag were exhibited for AoA smaller than 10° . Overall, the bumped blade provided greater advantage in lift to drag ratio (approximately 50%) over the AoA range from 0° to 20° . The sinusoidal leading edge also delayed the stall crisis, increasing the critical angle of attack by approximately 5° over the one for the blade with a straight leading edge.

1 Introduction

1.1 Design inspired by nature

Due to the rapid depletion of fossil fuels, and their / adverse effects on the environment, their cost has increased significantly during the past decades. This has emphasized the need for alternative energy

sources. Improving the conversion effectiveness of renewable energy into useful forms (like electricity) is also a priority. Site-specific optimization of wind turbines could improve the usage of wind energy [1], and this requires optimized blade design.

An investigation into aerodynamical effects of radical changes in the geometry of a turbine blade is presented in this paper. The aim was to examine the potential of improvements made to traditional blade

* Corresponding author. Tel.: +385 51 651 554; fax: +385 51 651 416

E-mail address: zoran.carija@riteh.hr.

designs by integrating a set of sinusoidal bumps into the leading edge (LE) of a conventionally straight-edged turbine blade.

Many technological breakthroughs come from interesting applications of innovative ideas and, in this case, the scientists discovered yet another possibility of mimicking nature as the bumped LE idea stems from tubercles — the characteristic protrusions on the pectoral fins of humpback whales. *Megaptera novaeangliae* are an endangered species of marine mammals. These baleen whales are extremely agile for their massive size, which is about 40 tons and 15 meters in length. While feeding, they can swim in a highly curved spiral path, sometimes in a tight diameter of less than 10 m. The secret of their agility is in their highly articulated pectoral fins, with characteristic tubercles on the leading edge that allow them great manoeuvrability when hunting plankton, krill and small shoals of fish [2]. This incredible hydrodynamic advantage can be considered a functional adaptation acquired through millions of years of natural selection of humpback whales and their evolution into the highly skilled hunters they are today. The bumps on their fins have only recently been the focus of research for possible applications in improved vortex generator design.

1.2 Paper outline

Since the efficiency of turbomachinery is largely determined by blade performance in the operational range, optimal blade design is crucial. The analogy between the hydrodynamic performance of pectoral fins of a humpback whale and the aerodynamics of a turbine blade can be used to design a blade that mimics the flow effects of fin tubercles [3].

Accordingly, fluid flow analyses of an isolated blade for a wide range of angles of attack (AoA) are presented.

Two types of blades have been analyzed. The first blade is a linear extrusion of an aerodynamic airfoil profile and has a smooth LE, while the second is based on similar cross-sections but has a sinusoidally curved LE inspired by the tubercles.

The assumption was that this curvature would affect the turbulent separation of the airflow from the blade, which would occur at a higher AoA , and in such a way that a greater lift force would be obtained.

Because of the irregular geometry and curvature of the bumped LE blade, and because of the dominant three-dimensional fluid flow effects near and in the wake area, it was necessary to conduct a 3D analysis of the flow. This approach provided a more accurate comparison of the two blades.

If the bumped LE blade should show better performance characteristics than the straight one, this kind of modification could find use in a great range of applications, i.e., airplane wings, helicopter rotors, fans, wind turbines, water turbines, etc.

1.3 Previous studies

There is extensive research into various airfoil designs that are differently suited for varying Reynolds numbers and angles of attack. Wind tunnel tests are the de facto method of validating numerical analyses of airfoil performance, Bruschi et al. [4]. Watts and Fish [5] simulated the flow over a wing equipped with bumps on the LE and one without them, both at large Reynolds numbers and different AoA . They found an improvement in performances for the wing with leading edge tubercles. For an AoA of 10° , the increase in resulting lift was 4.8%, while the reduction in drag was 10.9%. Lift to drag ratio increased by 17.6%.

Jen-Shiang Kouh et al. [6] investigated a NACA0012 airfoil with a chord length $c = 0.12$ m, equipped with varying sinusoidally shaped tubercles with sine amplitudes A ranging from $0.025c$ to $0.75c$ and sine wavelengths λ from $0.2c$ to $0.3c$. The results of their analyses, performed with a Reynolds number of $1.23 \cdot 10^5$, showed that the decrease in tubercles wavelength resulted in a critical AoA increase and that the decrease of tubercles amplitude increased the lift. Their wing reached a max critical AoA of 15° for the smallest wavelength ($0.02c$) and a maximum lift for the smallest amplitude, which is essentially the smooth LE wing.

Hansen et al. [7] made an experimental comparison between an unmodified NACA0021 airfoil and a similar one with tubercles of various amplitudes ($0.03c - 0.11c$) and wavelengths ($0.11c - 0.43c$), using the chord length c of 70mm. The Reynolds number was $1.2 \cdot 10^5$. The results of their experiment revealed that, for small Reynolds numbers, the foil with tubercles had a delayed stall, while the enhancement in performance was insignificant.

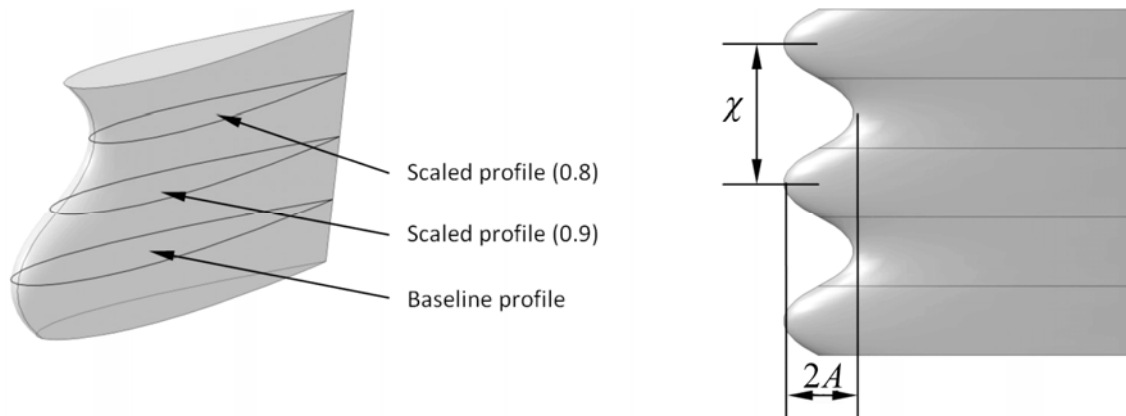


Figure 1. Definition of the bumped blade geometry showing wavelength χ and amplitude A .

They also concluded that the effectiveness of tubercles was very dependent on the Reynolds number.

Malipeddi [8] investigated the effects of a sinusoidal shaped LE of a NACA2412 airfoil in order to compare the results with those of a straight LE foil. The Reynolds number was $5.7 \cdot 10^5$, the chord length was $c = 0.1\text{m}$, the amplitudes were $0.025c$ and $0.05c$ and the wavelengths were $0.25c$ and $0.5c$. He made both a simulation and an experimental validation, the results of which more or less matched. His investigation showed that the wing with the shortest wavelength and the smallest amplitude has consistent characteristics for an AoA smaller than 12° , at which the separation begins and the wing stalls. For an AoA greater than 16° , the lift on the wing with tubercles was up to 48% greater and the drag up to 44% lower than on the ordinary wing. The results also revealed that the amplitude of the wing bumps significantly affected the performance for a greater AoA since the maximum lift was achieved at the optimum AoA by the conventional, straight LE wing.

2 Numerical model

2.1 Blade geometry and numerical mesh

This research analyses the impact of a bumped blade leading edge on the aerodynamic characteristics in an isolated flow field. The effects of bumps were determined by comparing specific numerical lift and drag characteristics between the bumped LE blade and the straight LE blade. The cross-sections of both blades were based on the NACA0012 airfoil profile.

Fig. 1 shows the definition of the bumped blade geometry. The bumped blade was combined from three scaled NACA0012 profiles mutually spaced vertically in a sinusoidal wave pattern to make tubercle-inspired bumps on the LE. The profile chord length was set at 100.7 mm for the largest one, the second and third were scaled at 0.9 and 0.8 chord length.

The resulting multisection surface created from those three profiles consisted of eight 40mm wide periodic blade segments attached together to form the endless bumped blade model shown in Fig. 2, which also shows a comparison of the leading edges of two blades: a) straight LE, b) bumped LE.

The dimensions of the straight LE blade were reduced to approximately 93% of those of the bumped LE blade so that equal blade surface areas could be obtained in both cases.

The final blade surface area measured in the modeler was 0.030 m^2 . Geometrical characteristics of both examined blades are listed in Table 1. The blade geometry was modeled using CATIA (Dassault Systems) and both blades were scaled to desired dimensions, positioned in such a way that their trailing edge was located at the coordinate system origin when imported into the Gambit pre-processor/mesher. Fig. 3 shows the computational domain used for simulation of fluid flow. Fig. 3a and 3b are shown using the coarsest of all tested numerical meshes (to provide a clearer view of resulting hexahedral volumes).

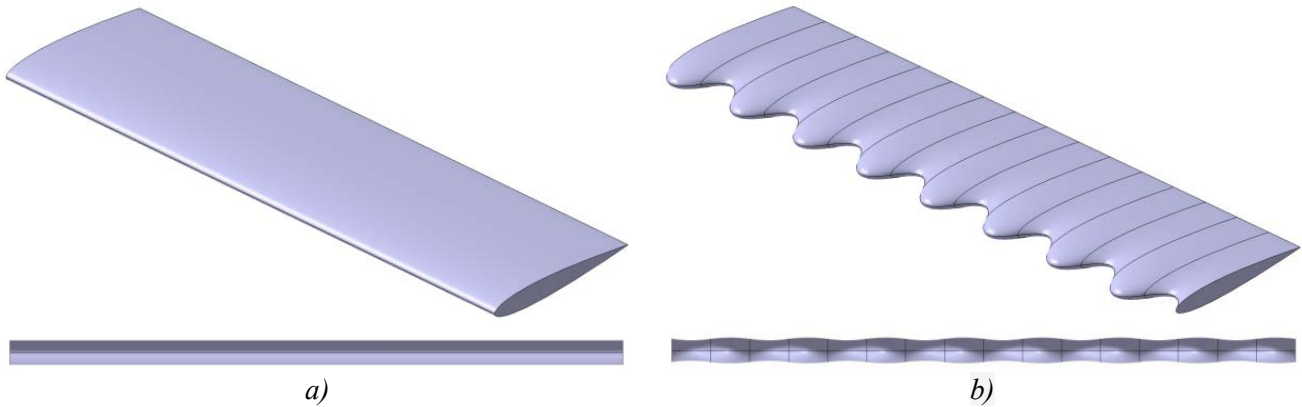


Figure 2. Leading edge of the two blade models: a) straight LE, b) bumped LE and surface.

Table 1. Geometrical characteristics of examined blades

	Straight LE blade	Bumped LE blade
Length of the blade profile	LB = 0.93545 Lchord	Lchord = 100.7 mm
Bump amplitude (A)	-	0.1 Lchord
Bump wavelength (χ)	-	0.397 Lchord
Repeated segment vertical length	320 mm	40 mm
Blade total vertical length	320 mm	320 mm
Blade surface area	0.030 m ²	0.030 m ²

The inlet section is located $12.5 \cdot L_{\text{chord}}$ upstream from the LE of the blade and the outlet section is located $30 \cdot L_{\text{chord}}$ away from the trailing edge (TE) of the blade in order to reduce reflecting disturbances from the outlet boundary. The upper and lower computational domain boundaries are located $12.5 \cdot L_{\text{chord}}$ away from the TE.

The computational domain was created using the Gambit (Fluent Inc. / Ansys.) preprocessor. Numerical meshes were generated using a C-type scheme of discretization, where the computational domain is described with reasonable numbers of hexahedral elements, i.e., a structured mesh. This results in the smallest size of the numerical mesh for a certain degree of solution accuracy.

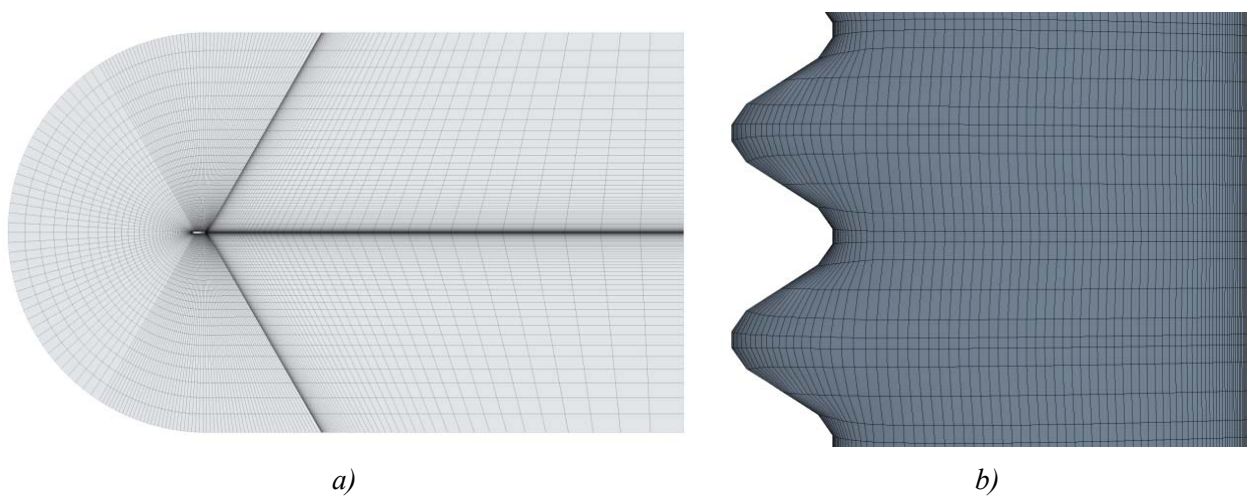


Figure 3. Numerical mesh displayed on; a) the upper wall, b) the blade surface.

The computational domain was divided into six sub-domains (Fig. 3a) to control the scheme application intended for a high quality numerical mesh with hexahedral elements as this would ensure a safe and fast solution convergence.

The C-type scheme offers a simple discretization control of the numerical mesh refinement (the number of control cells) and stretching factors allow for fine size adjustments of the first cell near the wall, which provides the value of Y^+ within the necessary range required by the turbulence model [9].

These refinements were first varied to find the numerical mesh with a minimum number of elements, ensuring a mesh independent solution. The chosen mesh contained 1 344 million volume cells. Ansys Fluent v6.3 was used to make a simulation of fluid flow around the blades.

The results obtained for the two blades were compared afterwards. The examined AoA were in the range from 0° to 30° with a 5° step.

2.2 Computational models

The commercial fluid flow solver used performs numerical analyses where governing equations are discretized using standard finite volume techniques. The mathematical model is simplified since it is assumed that the fluid flows without heat transfer. Turbulence is taken into account since the analyzed fluid flow falls into the high Reynolds-number where intensive fluctuations of the turbulent physical quantities occur. The simplest way of including turbulence is Reynolds averaging the governing equations. In this process, exact Navier-Stokes equations are transferred to the Reynolds-Averaged Navier-Stokes equations where the whole range of turbulence scales is modeled.

2.3 Conservation equations

After the Reynolds averaging approach for turbulence, an incompressible flow ($\rho = \text{const.}$) is modeled using the Navier-Stokes equations, which can be expressed as:

$$\frac{\partial \bar{v}_j}{\partial x_j} = 0 \tag{1}$$

$$\rho \frac{\partial (\bar{v}_i)}{\partial t} + \rho \bar{v}_j \frac{\partial (\bar{v}_i)}{\partial x_j} =$$

$$= -\frac{\partial \bar{p}}{\partial x_i} + \mu \frac{\partial^2 \bar{v}_i}{\partial x_j^2} + \frac{\partial \bar{p}}{\partial x_i} (-\rho \overline{v'_i v'_j}) \tag{2}$$

The Reynolds stress term is related to the mean velocity gradients by the Boussinesq hypothesis as:

$$-\rho \overline{v'_i v'_j} = \mu_t \left(\frac{\partial \bar{v}_i}{\partial x_j} + \frac{\partial \bar{v}_j}{\partial x_i} \right) - \frac{2}{3} \rho k \delta_{ij} \tag{3}$$

The standard $k-\varepsilon$ turbulence model with enhanced wall treatment was selected for turbulence closure. The solution-dependent dimensionless parameter Y^+ was used as a measure of numerical mesh quality during each simulation and was kept within recommended ranges on the blade wall zone.

2.4 Boundary conditions (BC)

The mesh in Fig. 3 shows the position of the blade relative to domain edges. Conditions selected for the domain boundaries during numerical analyses of fluid flow around both blade types were as follows.

The *velocity inlet* condition was selected for the rounded inlet section (left) and the components of velocity for each analyzed AoA were set respectively. The velocity magnitude was $v_m = 25\text{m/s}$. Turbulent kinetic energy and dissipation were defined using a turbulence intensity of 2% and the hydraulic diameter (the length of blade). The *outflow* boundary condition was selected at the rectangular outlet section (right). The blade surface was defined as non-porous, non-slip boundary where fluid velocity approaches zero and roughness. The remaining domain boundaries delimiting the volume of air around the blade were defined as non-periodic slip walls in order to reduce their influence on computed results.

The volume fluid definition used the standard properties of gaseous air selected from the solver database. Gravity was taken into account in the z-direction and the operating pressure was set to standard atmospheric pressure.

2.5 Convergence

The residuals and the values for the coefficients of lift and drag were monitored during all numerical analyses. The convergence criteria were satisfied when both the values of monitored residuals dropped below 10^{-5} , which is two orders of magnitude lower than standard convergence criteria,

and the computed values of lift and drag coefficients stabilized over subsequent iterations.

Typical changes in residuals and the coefficient of lift during iteration are shown in Fig. 4. It is evident that the convergence for this case was already achieved after 600 iterations.

3 Results

The lift and drag forces are two relevant variables to indicate the aerodynamic quality of a specific blade design. The efficiency of the blade is improved by increasing the lift and reducing the drag.

Designers usually grade the quality of a profile shape by the dimensionless lift coefficient C_L and drag coefficient C_D [10]:

$$C_L = \frac{L}{\frac{1}{2} \rho_{\infty} v_{\infty}^2 A} \quad (4)$$

$$C_D = \frac{D}{\frac{1}{2} \rho_{\infty} v_{\infty}^2 A} \quad (5)$$

where L is the lift force, D the drag force, A the area of the blade and v_{∞} the free stream velocity.

In order to evaluate the aerodynamic quality of the examined blades, Fig. 5 a) and 5 b) show a comparison of changes in drag and lift coefficients over a wide range of AoA for the bumped and straight LE blade, respectively. The choice between

the two types of blades would depend on the need for favourable lift/drag ratios either over the whole range, on average, or just the optimal region of AoA . From the data represented in Fig. 5 a), it can be concluded that, for an increasing AoA from the minimum 0° to about 10° , the lift coefficient constantly increases for both tested blades. The difference in computed lift coefficients between the blades is minimal, so it can be concluded that the application of bumps on the LE of the profile would have no positive impact in this area.

Since this range of AoA is specified as optimal or close to an optimal working area for turbomachines, it is important to note that the bumps on the blade LE have no significantly adverse impact on the lift coefficient in this area.

Increasing the AoA above 10° , up to the examined maximum of 30° , the positive impact of bumped LE comes into play. In this AoA range, the lift coefficient is 3% to 9.5% greater for the bumped blade in comparison to a straight blade.

As a consequence of using the $k-\varepsilon$ turbulent model, the computed values of lift for both blades show the occurrence of stall at a higher AoA than those obtained experimentally [11]. Better results should be expected using turbulent models with a higher level of accuracy, though this model was sufficient to demonstrate the advantages of a bumped LE.

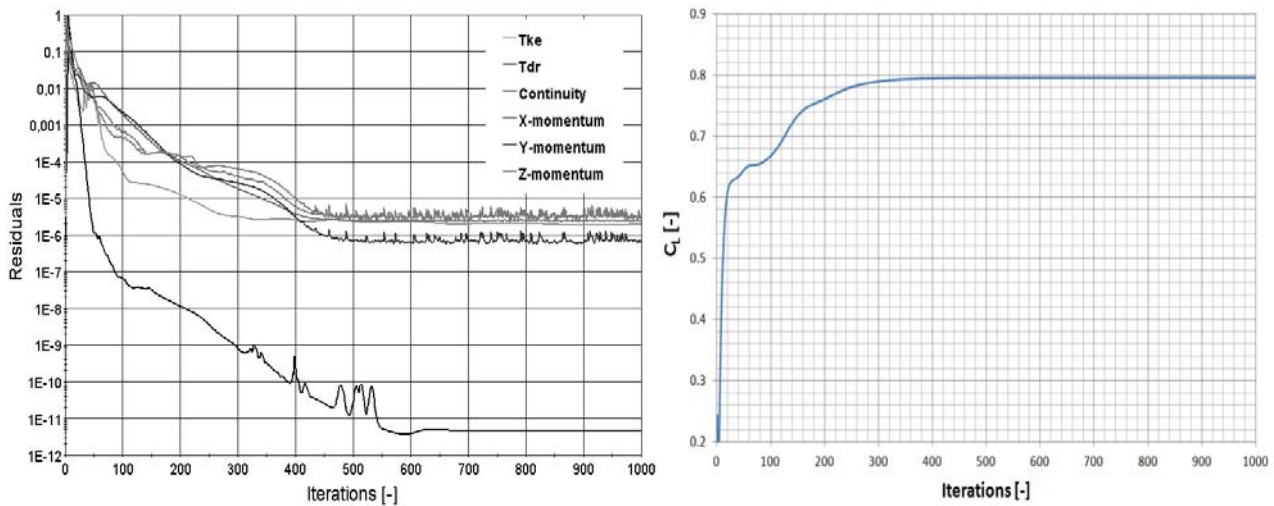


Figure 4. Convergence of residuals(left) and monitored values of lift coefficient (right) during iteration.

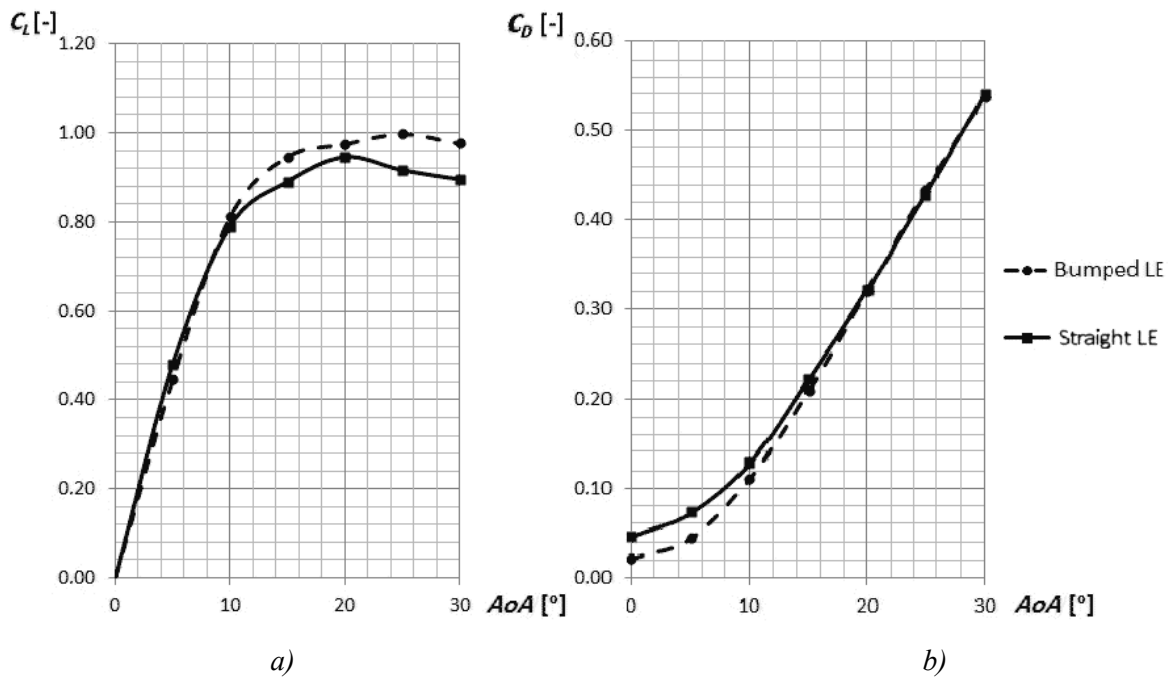


Figure 5. Coefficients a) lift C_L and b) drag C_D as curves for both blade LE types over the AoA range.

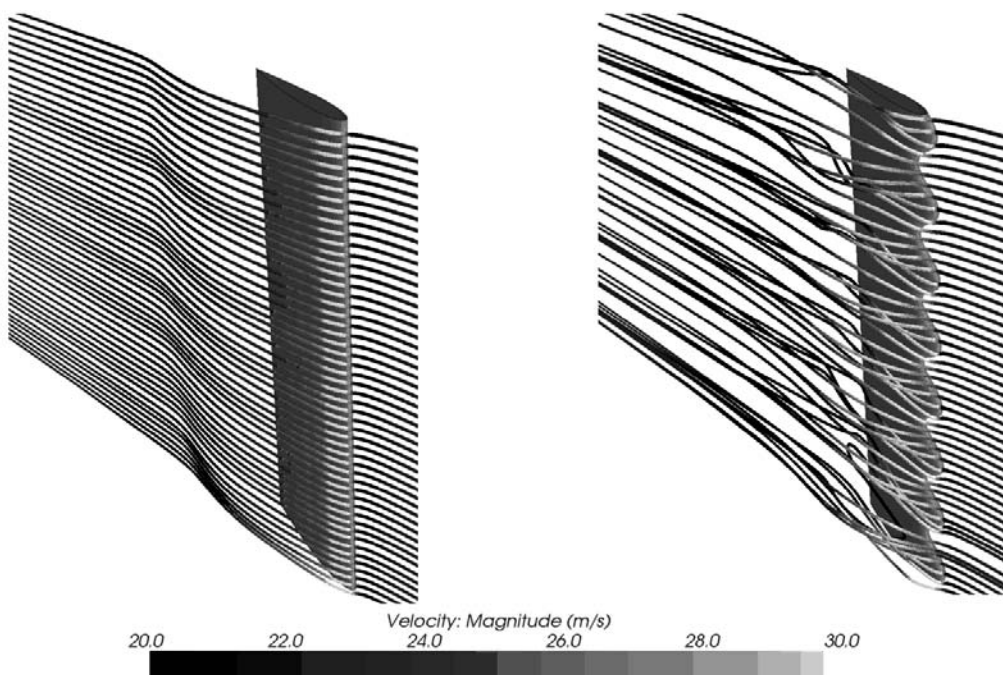


Figure 6. The flow around the blades at an AoA of 25°, shaded by velocity magnitude (ms^{-1}).

The comparison of drag coefficients in Fig. 6 b) shows that C_D is minimal for the lowest AoA (0°) and that its growth is positively proportional to the increase of AoA in both directions. In the AoA range from 0° to 15°, a smaller value of C_D was examined for the bumped blade. This would justify the use of

a bumped LE in the area of "optimal" AoA as the drag coefficient computed was up to 20% lower for the bumped blade than for the straight blade. Drag coefficients for the region above AoA 15° are very similar for both blades and the bumped blade provides no clear advantage in this aspect.

The CFD simulations that provided the integral characteristics of the analyzed problem also allow the visualization of computed fluid flow. Figure 6 shows the fluid flow path lines around the straight blade and the bumped blade, computed for the AoA of 25° . In both cases, the path lines are released from the same imaginary static line located 10 cm directly upstream from the blade LE, at a half of the total height of the domain.

Comparing the two images, a recirculation zone is observable at the blade suction side, which draws energy from the main stream, thus generating losses. It is interesting to note that the recirculation zone of the bumped blade is smaller than the one of the straight blade. This results in smaller losses and greater lift force and the next important advantage: a delay in stall occurrence. Figure 6 (left) shows the critical AoA (or stalling angle) at approximately 25° for the bumped blade, which represents a significant improvement over the straight blade that reaches it at 20° . Figure 6 (right) shows that the irregular shape of the LE has positive effects on the fluid flow. When the flow passes over a bump, two longitudinal vortices are formed that direct the fluid flow toward the suction-side of the blade as a consequence of the secondary rotational flow component. This characteristic of bumped LE blades causes a delayed stall crisis and better aerodynamical properties.

4 Conclusion

The assumption that the bumped shape of the leading edge (LE) of the humpback whale flippers, "designed" by the evolution of these cetaceans, has a beneficial effect on aerodynamic characteristics at high angles of attack (AoA) proved to be justified. Larger AoA on the fins of these mammals occur during feeding manoeuvres, when a sudden change of direction in motion is absolutely necessary for a successful feast.

In order to reproduce this, a broad range of AoA was examined to obtain a comparison of characteristics computed by simulating the fluid flow around an ordinary straight blade and the whale-inspired blade with a bumped LE, each isolated in a 3D flow field. The analysis showed that the calculated coefficient of lift C_L for the curved LE blade is overall higher for the examined AoA range (0° - 30°) except for a very narrow region at lower AoA where the straight LE blade had a higher lift coefficient as the fluid flow around the blade was optimal. The

predominantly better lift coefficient on the bumped blade is especially noticeable in regimes above an AoA of 10° where it is 3% to 9.5% greater than the one for the straight LE blade.

The improved lift coefficient of the bumped LE blade also shifted the stall crisis to a critical angle, approximately 5° greater than the one for the straight blade. The drag coefficient C_D for the bumped blade is not significantly lower in the tested region outside the optimum. The largest reduction in drag coefficient occurs for a small AoA where the more economical straight blade normally has an advantage in C_L .

Generally better characteristics of lift coefficients in the area above an AoA of 10° and better characteristics of the drag coefficients for the region of lower AoA demonstrate the influence of a bumped blade LE and show that it is an advantage over the ordinary straight blade. The improved aerodynamical characteristics of the bumped blade presented in this paper justify a deeper investigation of this kind of LE shape into rotary mechanical devices.

It would be necessary to examine the influence of the amplitudes and wavelengths of the bumps on the characteristics of the bumped LE blade design and to distinguish the relationship suitable for a particular flow regime as defined by the Reynolds number and other flow parameters. Rotor blades equipped with such curved LE shapes should raise the efficiency curve in the off-cam areas without compromising it in the optimal area. This should be experimentally verified on a purpose-built model, which could constitute the next step in our research. Flow measurements of prototypes in a wind tunnel would provide experimental results necessary for the comparison with numerical simulations in order to develop and perfect an economically viable design.

References

- [1] Schmidt, M.: *The Economic Optimization of Wind Turbine Design*, Thesis, Georgia Institute of Technology, 2007
- [2] Fish, F.E., Weber, P. W., Murray, M. M., Howle, L. E.: *The Tubercles on Humpback Whales' Flippers: Application of Bio-Inspired Technology*, Integrative and Comparative Biology, vol.51 no.1, 203-213, 2011

-
- [3] Canter, N.: *Humpback whales inspire new wind turbine technology*, STLE Tribology & Lubrication Technology, 2008
- [4] Bruschi, G., Nishioka, T., Tsang, K., Wang, R.: *Clark Y-14 Airfoil Analysis*, MAE Report, UCSD, California, 2003
- [5] Watts, P., Fish, F.E.: *The influence of passive, leading edge tubercles on wing performance*, Proceedings of the 12th International Symposium on Unmanned Untethered Submersible Technology, UUST01, Autonomous Undersea Systems Institute, Durham, NH, 2001
- [6] Kouh, JSh., Lin, HT., Lin, TsY., Yang, ChY, Nelson, B.S.: *Numerical Study of Aerodynamic Characteristic of Protuberances Wing in Low Reynolds Number*, National Taiwan Ocean University, Keelung, Taiwan, December 2011
- [7] Hansen, K. L., Kelso, R.M., Dally, B.B: *An investigation of Three-Dimensional Effects on the Performance of Tubercles at Low Reynolds Numbers*, School of Mechanical Engineering University of Adelaide, Australia, 2010
- [8] Malipeddi, A.K.: *Numerical analysis of effects of leading edge protuberances on aircraft wing performance*, Thesis, Wichita State University, 2011
- [9] Fluent 6.2 Documentation, *User's Manual*, Fluent Inc., 2005
- [10] Krause, A., Robinson, R.: *Improving Wind Turbine Efficiency through Whales-inspired Blade Design*, Harvey Mudd College Center for Environmental Studies, 2009.
- [11] Abbott, I.H., Von Doenhoff, A.E.: *Theory of wing sections*, Dover publications, Inc., New York, 1959

